4

Office of the Chief of Naval Research

Contract N00014-89-J-1276

Technical Report No. UWA/DME/TR-93-71

TWO-PARAMETER CRACK TIP FIELD ASSOCIATED WITH STABLE CRACK GROWTH IN A THIN PLATE —A HYBRID ANALYSIS

by

G. B. May, F. X. Wang And A. S. Kobayashi

April 1993

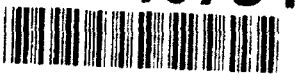

The research reported in this technical report was made possible through support extended to the Department of Mechanical Engineering, University of Washington, by the Office of the Chief of Naval Research under Contract N00014-89-J-1276. Reproduction in whole or in part is permitted for any purpose of the United States Government.

Department of Mechanical Engineering

College of Engineering

University of Washington

TWO-PARAMETER CRACK TIP FIELD ASSOCIATED WITH STABLE CRACK GROWTH IN A THIN PLATE - A HYBRID ANALYSIS

G.B. May, F.X. Wang and A. S. Kobayashi
University of Washington
Department of Mechanical Engineering
Seattle, Washington 98195, USA

ABSTRACT

Moiré interferometry was used to determine the two orthogonal displacement fields surrounding a stably growing crack in a thin 2024-T3 aluminum alloy, single-edge notched (SEN) specimen. The measured displacements were used to compute the J-integral and the associated HRR and the second order Q displacement fields. Also a 2-D elastic-plastic finite element model of the fracturing specimen was executed in its generation mode to compute the crack tip displacement field and the J-integral for small crack extension. The numerically computed and experimentally derived J-values agreed prior to crack extension but differed increasingly with stable crack growth. The HRR and measured v-displacements agreed well but significant difference between the HRR and measured u-displacements was noted. Thus the Q component of the v-displacement was negligible but the corresponding u-component varied nonlinearly with radial distance from the crack tip.

INTRODUCTION

A hybrid experimental-numerical procedure using the displacement field obtained by geometric moiré technique to drive elastic-plastic, 2-D and 3-D finite element codes was first demonstrated by Hareesh and Chiang [1]. In their analysis, experimental surface displacements were used to compute the interior two- and three-dimensional displacements and strains in a plastically deforming stationary notch tip of a 3.2-mm thick, 6061-T6 aluminum alloy, single edge notched (SEN) specimen. The authors concluded that a ten fold saving in computer processing time was achieved through their hybrid analysis and that their 3-D hybrid model showed significant three dimensional effects, which otherwise could not be detected by surface displacement measurements alone, in the very vicinity of the notch tip.

With the increasing use of an order-of-magnitude more sensitive moiré interferometry, it was inevitable that it be incorporated into the above hybrid analysis. Sivaneri et al [2] used the displacement fields obtained by a white-light moiré interferometry of a 2024-0, 0.8-mm thick, fatigue precracked SEN specimen [3] to drive an elastic-plastic, plane stress finite element code. Among other numerical results, the J-

integral value and the associated HRR displacement field [4,5] at the initial stage of loading were computed. The latter was in excellent agreement with the two orthogonal measured displacements.

In recent years, one of the authors and his colleagues have been using the orthogonal, crack tip displacement field provided by moiré interferometry to determine the J-integral value and the associated HRR crack tip displacement field surrounding a stably growing crack in thin, 2024-0, 2024-T3, 5052-H32 and 2091-T3 aluminum alloy SEN specimens [6-8]. These experimental results showed that these J-integral values differed substantially with previously published solutions [9,10] in the presence of large scale yielding and were not path independent after a moderate stable crack growth of 5 mm. Also the HRR displacement field, which was computed by using the measured J-integral value, did not agree with the measured displacement field for submillimeter crack growth. These conclusions were unexpected since both the J-integral and the HRR field had been studied in detail and had been repeatedly verified through many numerical investigations. These results also suggest that perhaps the fault lies in the elastic-plastic finite element codes based on deformation/incremental plasticity with isotropic/kinematic strain hardening. Furthermore, the slope of the log-log plots of the second order Q displacement components varied irregularly with no consistent second order strain singularity.

The purpose of this paper is to compare the elastic-plastic fracture parameters, obtained from a commercially available 2D finite element code with those obtained experimentally surrounding a stably growing crack in a thin fracture specimen. Since the existing 2D finite element codes generally predict the overall elastic-plastic response of a structure with reasonable accuracy, this study focuses on the ability of a code to accurately compute the J-integral and the crack tip displacements. Thus the FEM code will be confined to a local region, surrounding the crack tip, by prescribing the measured displacements along a remote boundary of this stationary region.

TWO-PARAMETER CRACK TIP STRESS FIELD

The two-parameter representation of the elastic-plastic crack tip stress field has been discussed by Li and Wang [11], Sharma and Aravas [12] and Yang, Cho and Sutton [13]. This plane strain, asymptotic stress field is based on the J_2 deformation theory with the following power hardening material of Ramberg-Osgood:

$$\varepsilon_{ij} = \frac{1+\nu}{E}\, s_{ij} + \frac{1-2\nu}{3E}\, \sigma_{kk}\delta_{ij} + \frac{3}{2}\, \alpha\varepsilon_o \left(\frac{\sigma_e}{\sigma_o}\right)^{n-1} \frac{s_{ij}}{\sigma_o} \qquad (1)$$

where i, j = 1 or 2 corresponds to a Cartesian coordinate system with axes parallel or perpendicular to the crack, respectively, E and n are the modulus of elasticity and Poisson's ratio respectively, σ_o and ε_o are the yield stress and strain, respectively, α and n are material constants and σ_e and s_{ij} are the equivalent and deviatoric stresses, respectively. The existence of the following asymptotic expansion of the crack tip solution was then postulated and represented in terms of the equivalent stress as

$$\frac{\sigma_e(r,\theta)}{\sigma_o} = r^s \sigma_e^{(o)}(\theta) + r^t\, \sigma_e^{(1)}(\theta) + \cdots \qquad \text{as } r \to 0 \qquad (2)$$

A J-integral is then used to determine the leading order exponent of s = -1/(n+1) and to no surprise the HRR crack tip field [4] is recovered from the first term in Equation (2). The order of magnitude of the second term in Equation (2) depends on the second exponent, t. In particular, when t = 0 for the second and all higher order terms, the simplified Q stress component of [14,15] is recovered.

Based on extensive numerical analysis, O'Dowd and Shih [14] suggested the following two-term approximation to Equation (2) in terms of a polar coordinate at the crack tip as

$$\frac{1}{\sigma_o}\begin{pmatrix}\sigma_{rr} & \sigma_{r\theta}\\ \sigma_{r\theta} & \sigma_{\theta\theta}\end{pmatrix} = \left(\frac{J}{\alpha\varepsilon_o\sigma_o I_n r}\right)^{(1/n+1)}\begin{pmatrix}\tilde{\sigma}_{rr} & \tilde{\sigma}_{r\theta}\\ \tilde{\sigma}_{r\theta} & \tilde{\sigma}_{\theta\theta}\end{pmatrix} + Q\left(\frac{r}{J/\sigma_o}\right)^t\begin{pmatrix}\tilde{\sigma}_{rr} & \tilde{\sigma}_{r\theta}\\ \tilde{\sigma}_{r\theta} & \tilde{\sigma}_{\theta\theta}\end{pmatrix} \tag{3}$$

where J is Rice's J-integral, Q is a dimensionless constant that controls the magnitude of the second stress term and $I_n = I_n(q)$ is tabulated in Reference [16]. Equation (3) is specifically restricted to the forward sector of the crack tip.

O'Dowd and Shih further reasoned that since $\tilde{\sigma}_{rr} = \tilde{\sigma}_{\theta\theta}$ and $|\tilde{\sigma}_{r\theta}| << |\tilde{\sigma}_{\theta\theta}|$, Q is essentially a plane strain, stress triaxiality parameter which could include the influence of all higher order terms in Equation (2) [14]. The strain and displacement components corresponding to this plane strain Q component are then a hydrostatic strain and a linearly varying homogeneous displacement, respectively.

For the state of plane stress, Reference [12] shows that the second order stress component of $\sigma_e^{(1)}$ in Equation (2) approaches infinity as $\theta \rightarrow 160^\circ$ and thus the second order solution probably is not separable. In the region of $\theta < 140^\circ$, however, $\sigma_e^{(1)}$ variation is normal and thus one can speculate that the two parameter stress expression holds within this restriction, or specifically in the forward section of the crack tip as noted in Reference [14]. This hypothesis is important if the two-parameter J-Q theory is to be used in characterizing ductile fracture of thin plates where a 100 percent shear lip with no cleavage fracture is anticipated.

The strain and the displacement components corresponding to the above two term representation of Equation (3) can be represented in a nondimensional form as [14]

$$\frac{\varepsilon_{ij}}{\alpha\varepsilon_o} = \left(\frac{J}{\alpha\varepsilon_o\sigma_o I_n r}\right)^{n/(n+1)}\tilde{\varepsilon}_{ij}^{(0)}(\theta) + Q\left(\frac{r}{J/\sigma_o}\right)^t\left(\frac{J}{\alpha\varepsilon_o\sigma_o I_n r}\right)^{(n-1)/(n+1)}\tilde{\varepsilon}_{ij}(\theta) \tag{4}$$

$$\frac{u-u^o_i}{\alpha\varepsilon_o} = \left(\frac{J}{\alpha\varepsilon_o\sigma_o I_n}\right)^{n/(n+1)} r^{1/(n+1))}\,\tilde{u}^{(0)}(\theta) + Q\left(\frac{r}{J/\sigma_o}\right)^t\left(\frac{J}{\alpha\varepsilon_o\sigma_o I_n}\right)^{(n-1)/(n+1)} r^{2/(n+1)}\,\tilde{u}^{(1)}(\theta) \tag{5}$$

A-1

where u^o_i is the rigid body displacement.

In the following, the possibility of extending the plane strain, two-parameter characterization of a stationary ductile crack to large stable crack growth problems in thin plates is investigated. Specifically, the experimentally determined crack tip displacement field in a thin plate specimen with that predicted by the J-Q theory is compared. Only a qualitative comparison is possible since the second order term in Equation (6) could not be computed as $\tilde{u}^{(1)}(q)$ is not known for the state of plane stress.

EXPERIMENTAL ANALYSIS

Experimental Procedure

The orthogonal displacement components surrounding the crack tip were measured by moiré interferometry using relatively coarse, cross diffraction grating of 40 lines/mm. This coarse grating was necessary due to the gross yielding and the large strain components, which will generate a moiré fringe pattern too dense to resolve, associated with the large stable crack growth in a ductile specimen. The coarse, crossed diffraction grating was transferred onto the specimen surface using photoresist and is similar to the procedure developed by Ifju and Post [17]. However, in this study, the highly polished surface of the aluminum specimen provided sufficient reflectivity and thus an evaporated aluminized coating was not used. This reflective specimen surface also eliminates the loss of moiré fringes at high strain where an aluminized coating craze and obliterate the diffraction grating.

The specimen was then illuminated by a four beam moiré interferometer [18] for simultaneous recording of the two orthogonal displacement fields. Figure 1 shows the moiré interferometry setup and the u-v mirror arrangement used in this study. The coarse diffraction grating reduced the incident angle of the four beams thus simplifying the u-v mirror supports.

Specimen

The specimen consists of a fatigue precracked, thin single-edged notch (SEN), 2024-T3 aluminum alloy specimen shown in Figure 2. The moiré diffraction grating covered a region of 25.4 x 50.8 mm surrounding the crack as shown. The SEN specimen was subjected to uniaxial tensile loading in a displacement controlled testing machine and the moiré interferometry patterns were recorded at various stages of stable crack growth.

NUMERICAL ANALYSIS

A commercial finite element code was used to compute the elastic-plastic state associated with stable crack growth in this specimen. The objective of this numerical analysis was to generate numerical results, which can be compared with the experimental results, at various stages of stable crack growth with large scale yielding. In practice however, the available code could only handle modest plastic straining associated with a small stable crack growth of $\Delta a = 1.5$ mm before collapsing.

Unlike traditional finite element method (FEM), the measured displacements near the boundary of moiré grating were used as input boundary conditions to the FEM model

of the SEN specimen. As described in [1,2], this procedure not only results in saved computer time but provides detailed information, which is lacking in the moiré analysis particularly at the initial stage of stable crack growth, in the immediate vicinity of the crack tip. Also, as described in [1,2], this load path dependent, elastic-plastic finite element analysis must start from the early stage of plastic yielding and proceed incrementally along the loading path.

Figure 3 shows the finite element model used in this analysis. The power hardening stress-strain relation used in this incremental elastic-plastic analysis was that of Dadkhah [19]. Also due to the sensitivity of the FEM to a displacement-prescribed boundary condition, a second order curve, which was fitted to the measured boundary displacements obtained from moiré interferometry, was used as the input boundary condition.

RESULTS

A total of nine increments of load, as shown in Figure 4, were applied and the corresponding moiré interferometry fringes were recorded. Figure 5 shows typical moiré fringe patterns corresponding to the displacement parallel, u, and perpendicular, v, to the crack. Also shown in Figure 5 are the rectangular contours used for the J-integral computation [19]. This computation, using moiré interferometry data, was conducted only for the latter stages of loading with more dense moiré fringe patterns.

Figure 6 shows the various J-values with crack extension computed by the build in algorithm of the commercial FEM code used, J_{FEM}, and through contour integration [6,7,8] using the moiré fringe data, J_{exp1} and J_{exp2}. J_{FEM} computation had to be terminated at Δa = 1.5 mm due to the large distortion of the small finite element surrounding the crack tip. The equivalent elastic J-value was obtained by setting J = G (strain energy release rate), J_{LEFM}, and J_{Shih} was computed using the procedure and tables in [9,10]. J_{exp1} and J_{exp2} differ by the size of contour with former being 5 x 5 mm and the latter was 10 x 10 mm. The differences in the theoretical, experimental and numerical results essentially follow the same trend in [6,8]. It is interesting to note that both J_{FEM} and J_{Shih} are relatively close and both differ substantially with J_{exp1} and J_{exp2}.

Figure 7a shows log-log plots of the measured v-displacements, the computed HRR and the |Q| components of the v displacements along the radial line of $\theta = 45°$ for a stable crack growth of Δa = 1.5 mm. Here |Q| is the absolute value of the difference between the experimental and HRR displacement components and is not the Q value in Equation (5). The measured v displacements and the HRR components of the v displacements nearly coincide for $r\sigma_o/J > 10$ but differs substantially for $r\sigma_o/J \approx 1$. The |Q| component of the v displacements is an order of magnitude smaller and possibly within the error band of the measurement.

Figure 7b shows the corresponding log-log plot of the measured u-displacement and the computed HRR and the |Q| components of the u displacement. For $r\sigma_o/J \approx 10$ the |Q| components is the same order of magnitude as the measured u displacement and the corresponding HRR component and varies approximately as $r^{-1.1874}$ for r = 1 mm. This exponent indicates that the corresponding normal strain component is nearly a constant independent of r and is closer to the T-component as predicted by the J-T theory [20].

Figures 8a and 8b show the log-log plots of the measured, computed HRR and Q component of the v- and u-displacements, respectively for a large crack extension of Δa = 3.9 mm. While the HRR and measured v-displacements for $r\sigma_o/J = 10$ are in reasonable agreement despite the large crack extension, significant difference is noted in the u-displacement. The associated Q component is negligible for the v-displacement but increases by $r^{0.44}$ for the u-displacement. Thus, for this larger Δa = 3.9 mm, neither the J-Q nor the J-T theories appears to be applicable.

DISCUSSION

The $\tilde{u}^{(1)}$, $\tilde{\varepsilon}^{(1)}$ and $\tilde{\sigma}^{(1)}$ functions are yet to be determined for the state of plane stress assuming that the stresses are separable into functions of r and θ. The negligible |Q|-component of the v-displacement and the slope of the |Q|-component of the u-displacement for small stable crack growth suggest that the J-T theory may account for the cummulated effects of the higher order terms in Equation (2).

CONCLUSIONS

A comparison of experimentally determined crack tip displacement fields in a thin SEN specimen with predictions by the J-Q theory has been carried out. The comparison is qualitative since the form of the J-Q displacement fields is not known for plane stress.

Limited experimental results involving the crack tip displacement fields in thin aluminum SEN with small stable crack growth showed that the J-Q, based on the plane strain form, may not be present. On the other hand, the simpler J-T crack tip field [20] could exist.

Also, the use of the present J-integral computation procedures using [9] and a commercial code for elastic-plastic fracture analysis of thin plates in the presence of stable crack growth must be reinvestigated in view of the observed large discrepancies.

ACKNOWLEDGMENTS

This research was supported by the Office of Naval Research under ONR Contract N00014-89-J-1276. The authors are indebted to Dr. Yapa D.S. Rajapakse for his support during the course of this investigation.

REFERENCES

1. Hareesh, T.V and Chiang, F.P. "Integrated Experimental-Finite Element Approach for Studying Elasto-Plastic Crack-Tip Fields," *Engineering Fracture Mechanics*, vol. 31, No. 3, pp. 451-461, 1988.

2. Sivaneri, N.T., Xie, Y.P. and Kang, B. S.-J., "Elastic-plastic Crack-Tip-Field Numerical Analysis Integrated with Moire Interferometry," *International Journal of Fracture*, vol.49, pp. 291-303, 1991.

3. Kang, B. S.-J., "Experimental Investigation of Ductile Fracture by White Light Moire Interferometry," PhD dissertation, University of Washington, Seattle, 1987.

4. Hutchinson, J.W., "Plastic Stress and Strain Fields at a Crack Tip, " *Journal of Mechanics and Physics of Solids*, vol. 16, pp. 13-31, 1968.

5. Rice, J.R. and Rosengren, G.F., "Plane Strain Deformation Near a Crack Tip in a Power Hardening Material," *Journal of Mechanics and Physics of Solids*, vol. 16, pp. 1-12, 1968.

6. Dadkhah, M.S., Kobayashi, A.S. and Norris, W.L., "Crack Tip Displacement Fields and J-R Curves of Four Aluminum Alloys," Fracture Mechanics: Twenty-second Symposium (Volume II), ASTM STP 1131, S.N. Atluri, J.C. Newman, Jr., I.S. Raju and J.S. Epstein, eds., *American Society for Testing and Materials*, Philadelphia, pp. 135-153, 1992.

7. Dadkhah, M.S. and Kobayashi, A.S., "Further Studies in the HRR Field of a Moving Crack, An Experimental Analysis," *International Journal of Plasticity*, vol. 6, pp. 635-650, 1990.

8. Dadkhah, M.S. and Kobayashi, A.S., "Two-parameter Crack Tip Field Associated with Stable Crack Growth in a Thin Plate - An Experimental Analysis," to be published in *Fracture Mechanics: Twenty Fourth Symposium*, ASTM.

9. Kumar, V., German, M.D. and Shih, C.F., "An Engineering Approach for Elastic-Plastic Fracture Analysis," *Electric Power Research Institute Tropical Research*, NP-1931, Research Project 1237-1, July 1981.

10. Shih, C.F., German, M.D. and Kumar, V., "An Engineering Approach for Examining Crack Growth and Stability in Flawed Structures," *International Journal of Pressure Vessel and Piping*, vol. 9, pp. 159-196, 1981.

11. Li, Y and Wang, Z., "Higher Order Asymptotic Field of Tensile Plant Strain Nonlinear Crack Problems," *Scientia Sinica* (Series A), vol. 29, pp 942-955, 1986.

12. Sharma, S.M. and Aravas, N., "Determination of Higher-Order Terms in Asymptotic Crack Tip Solutions," *Journal of Mechanics and Physics of Solids*, vol.39, No. 8, pp 1043-1072, 1991.

13. Yang, S., Chao, Y.J. and Sutton, M.A., 'Higher Order Asymptotic Crack Tip Fields in a Power Hardening Material," to be published in Engineering Fracture Mechanics.

14. O'Dowd, N.P. and Shih, C.F., "Family of Crack-Tip Fields Characterized by a Triaxiality Parameter: Part I - Structure of Fields," *Journal of Mechanics and Physics of Solids*, vol. 39, No. 8, pp 989-1015, 1991.

15. O'Dowd, N.P. and Shih, C.F., "Two-Parameter Fracture Mechanics: Theory and Applications," to be published.

16. Shih, C.F., "Tables of Hutchinson-Rice-Rosengren Singular Field Quantities," *MRL E-147*, Materials Research Laboratory, Brown University, June 1983.

17. Ifju, P. and Post, D., "Zero-Thickness Specimen Gratings for Moire Interferometry," *Experimental Techniques*, vol.15, no.2, pp. 45-47, March/April 1991.

18. Guo, Z.K. and Kobayashi, A.S., "Simultaneous Measurement of U and V-Displacement Fields by Moire Interferometry," to be published in *Experimental Techniques*.

19. Dadkhah, M, and Kobayashi, A.S., "HRR Field of a Moving Crack, an Experimental Analysis," *Engineering Fracture Mechanics*, vol. 33, pp.253-262, 1989.

20. Betegon, , C. and Hancock, J.W., "Two-Parameter Characterization of Elastic-PlasticCrack Tip Field," *ASME Journal of Applied Mechanics*, vol. 58, 104-110 (1991).

ASK/cm/4/22/93/ONR/TR93-71

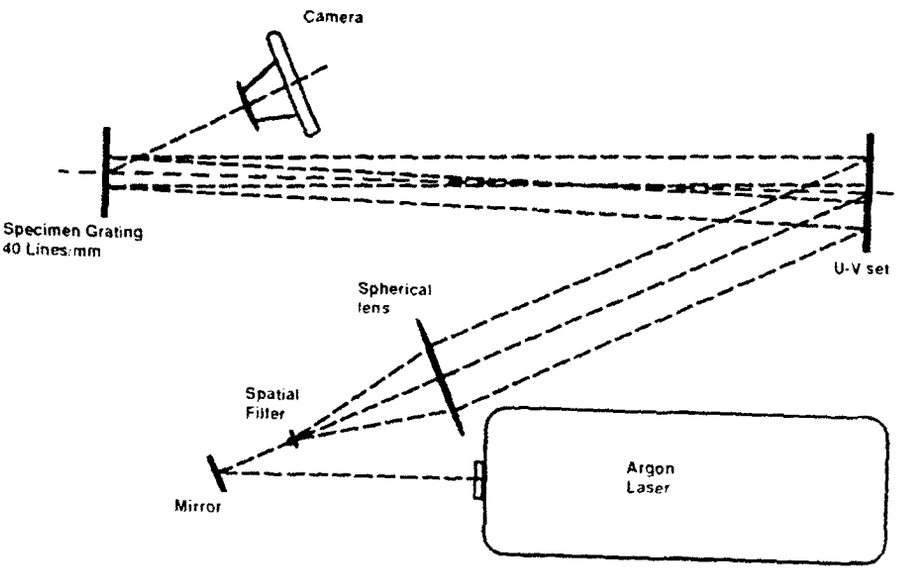

(a) Optical setup

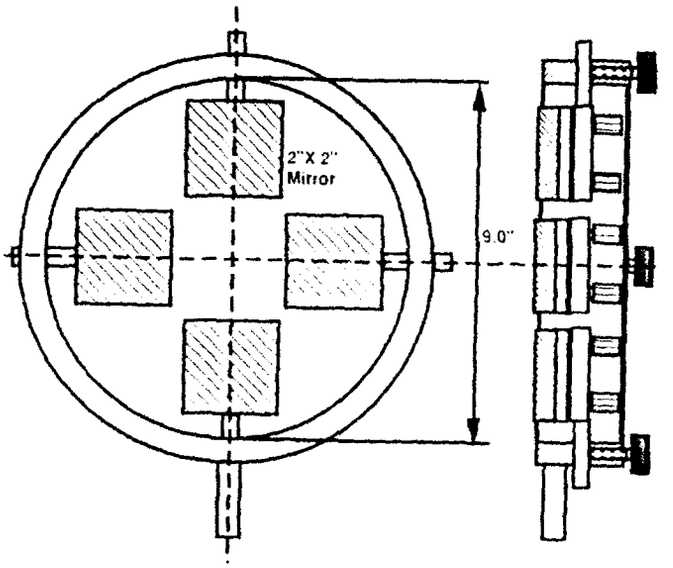

(b) Small u-v setup

Fig. 1 Moiré interferometry setup.

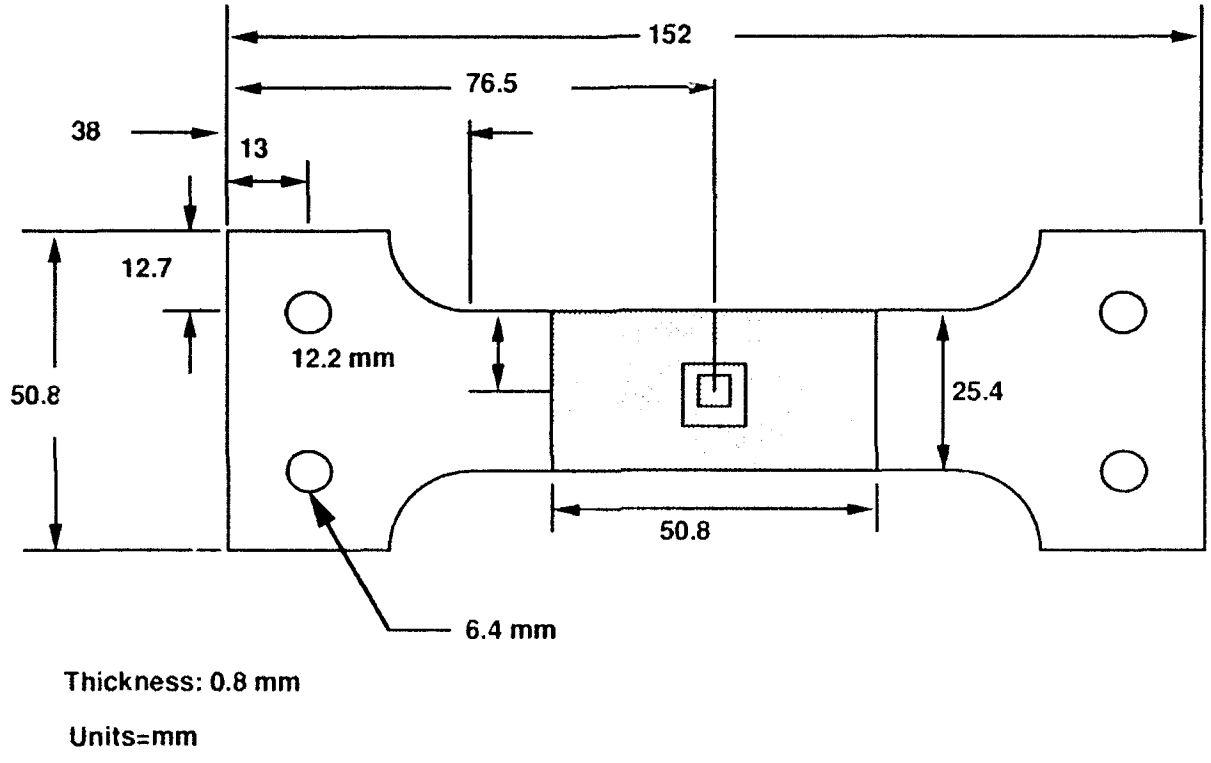

Fig. 2. SEN 2024-T3 aluminum alloy specimen with J-integral contours.

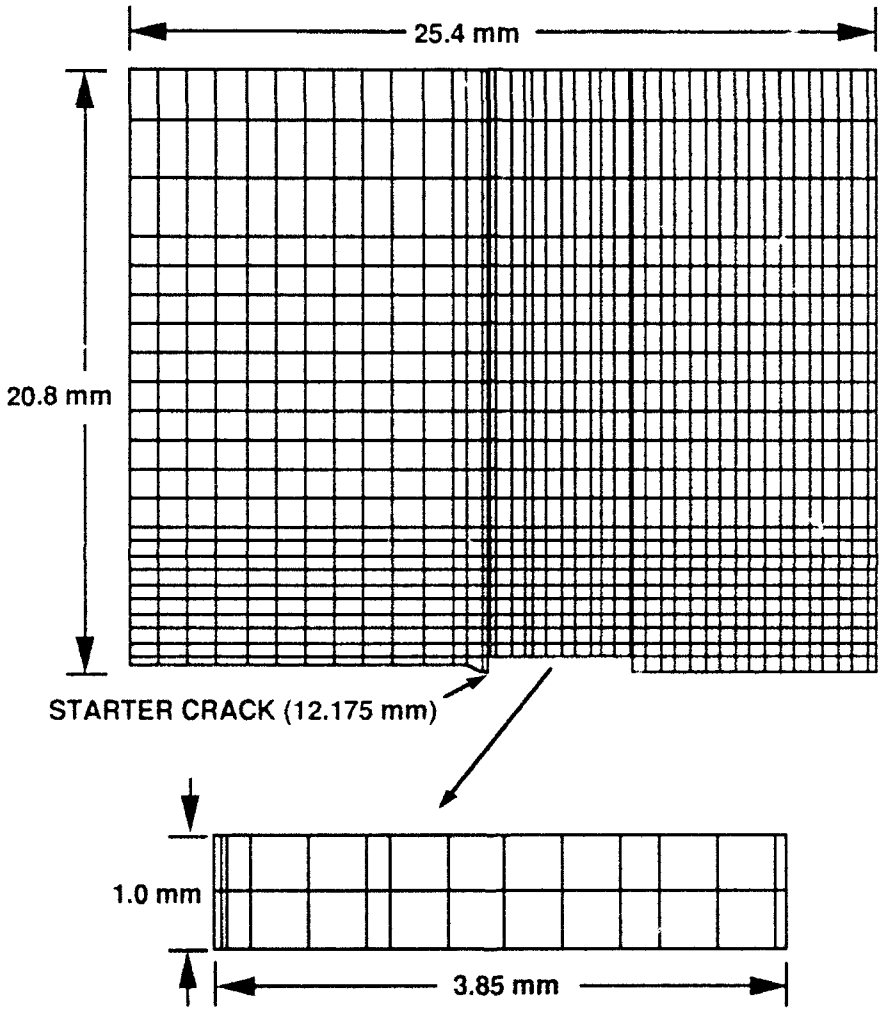

Fig. 3 Finite element mesh used in elastic-plastic analysis.

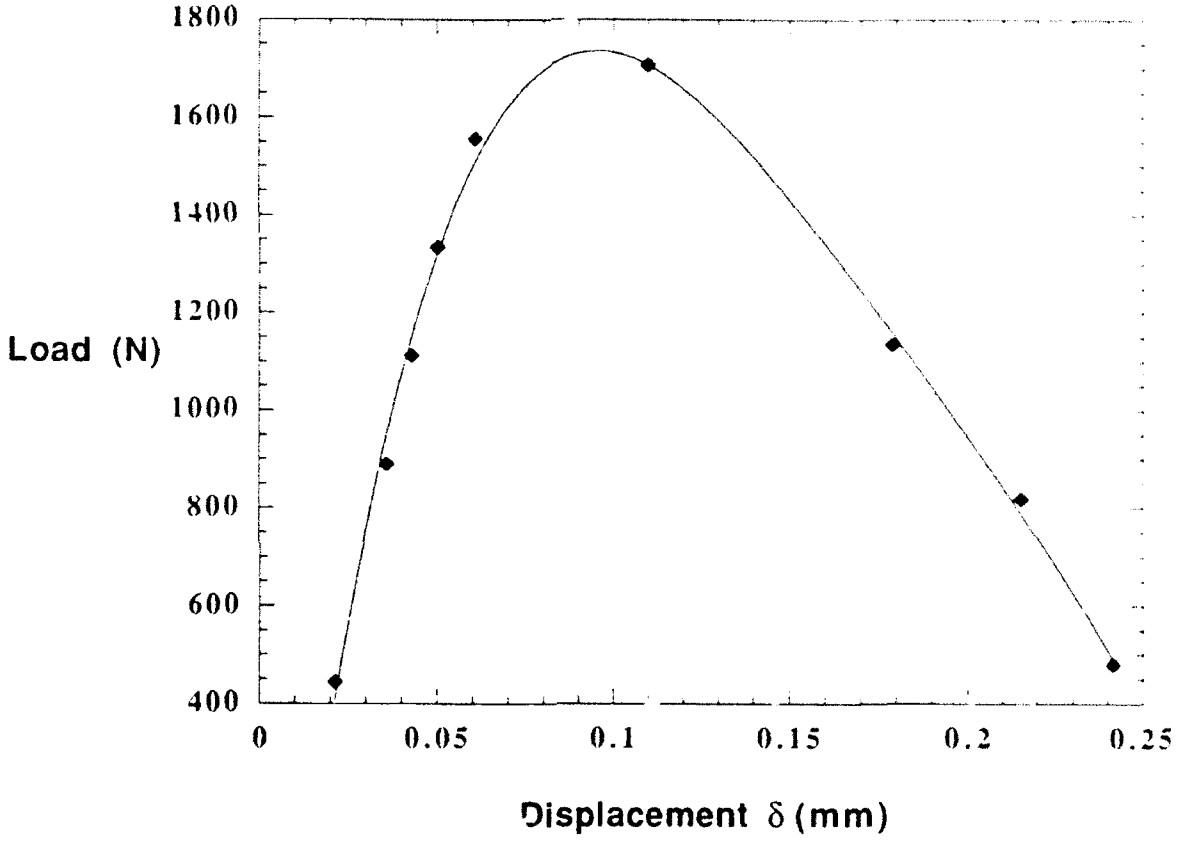

Fig. 4. Applied load vs. load line displacement for 2024-T3 SEN specimen.

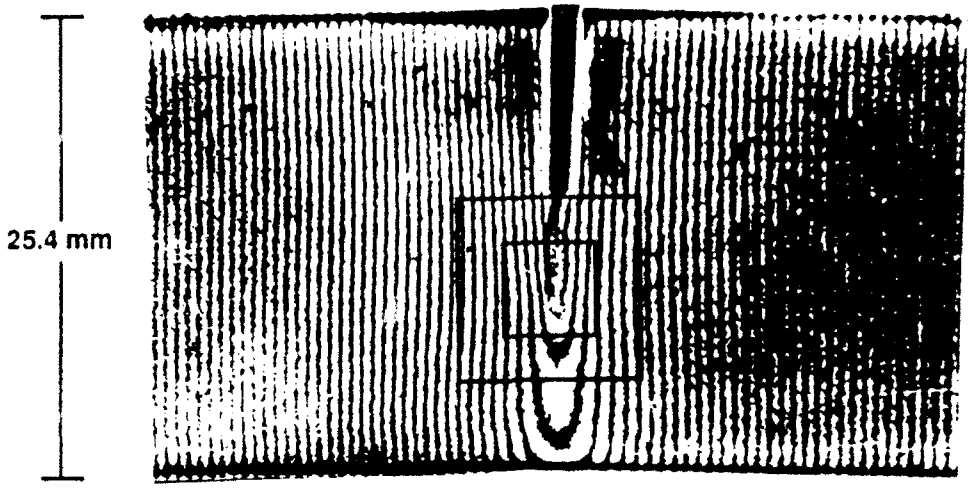

u-displacement field

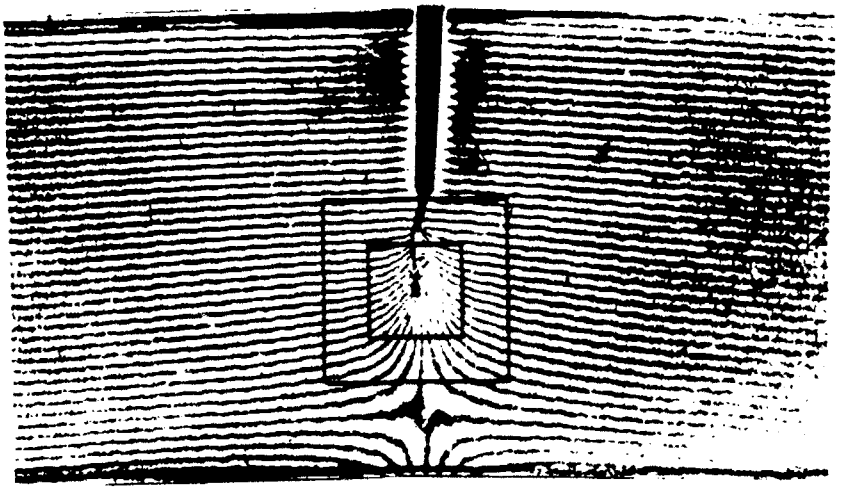

v-displacement field

Fig. 5 Moiré patterns of the 2024-T3 specimen with contours [Load = 1134 (N)].

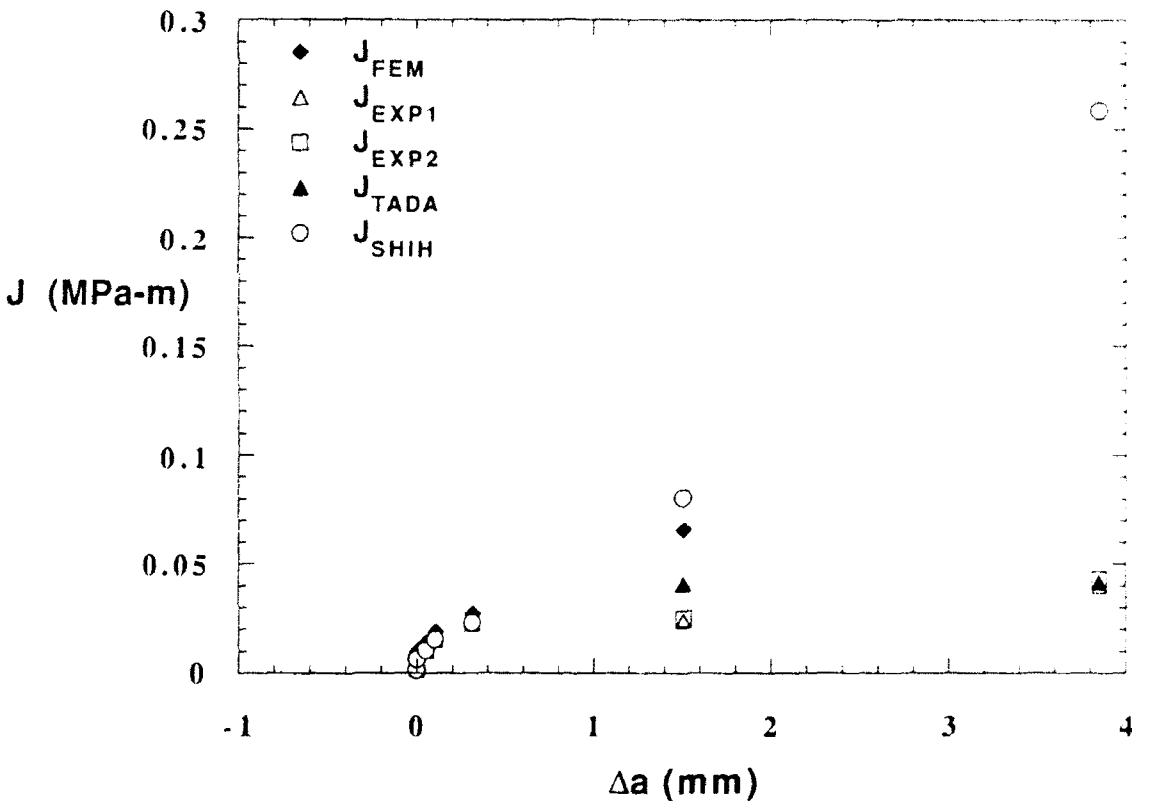

Fig. 6. J-integral for 2024-T3 SEN specimen.

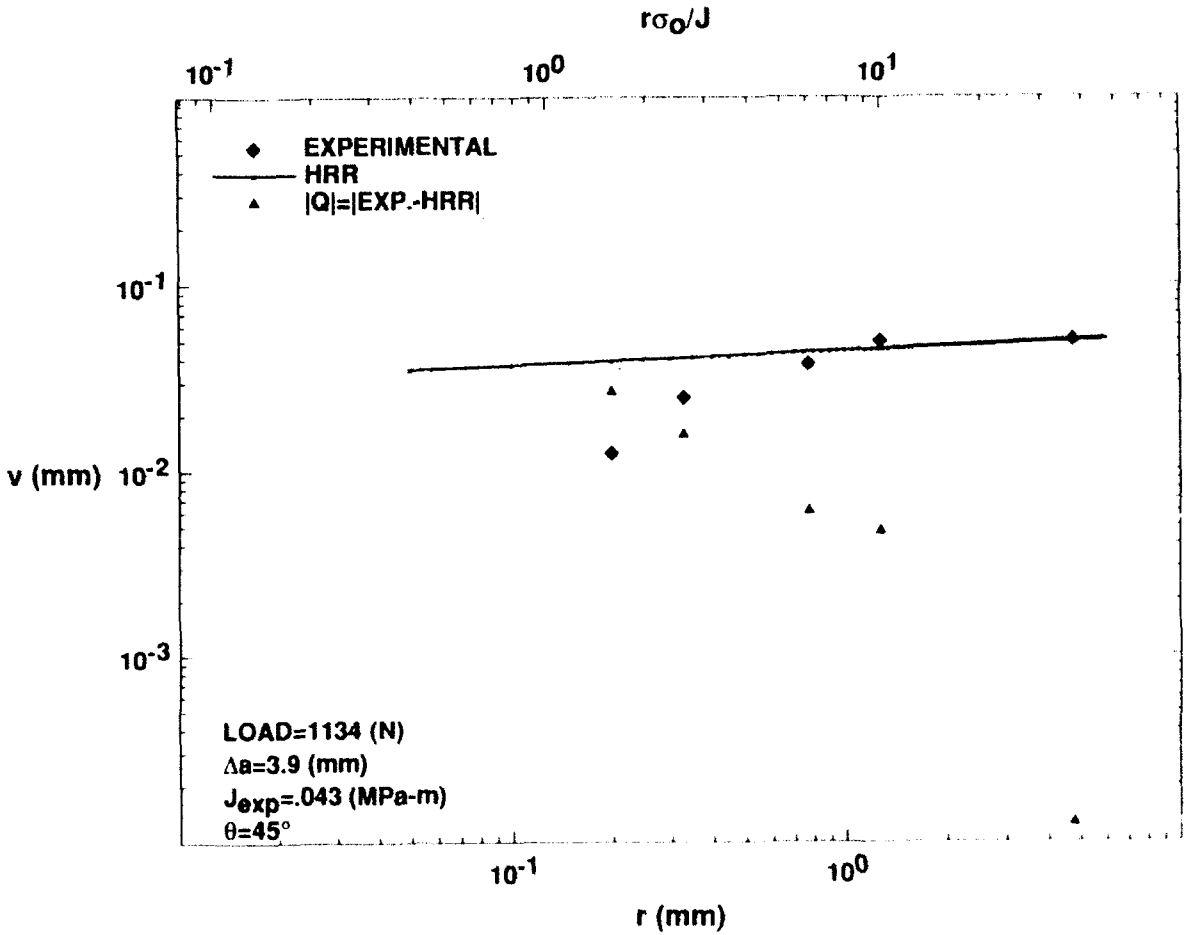

Fig. 7a. v-displacement in 2024-T3 SEN specimen.

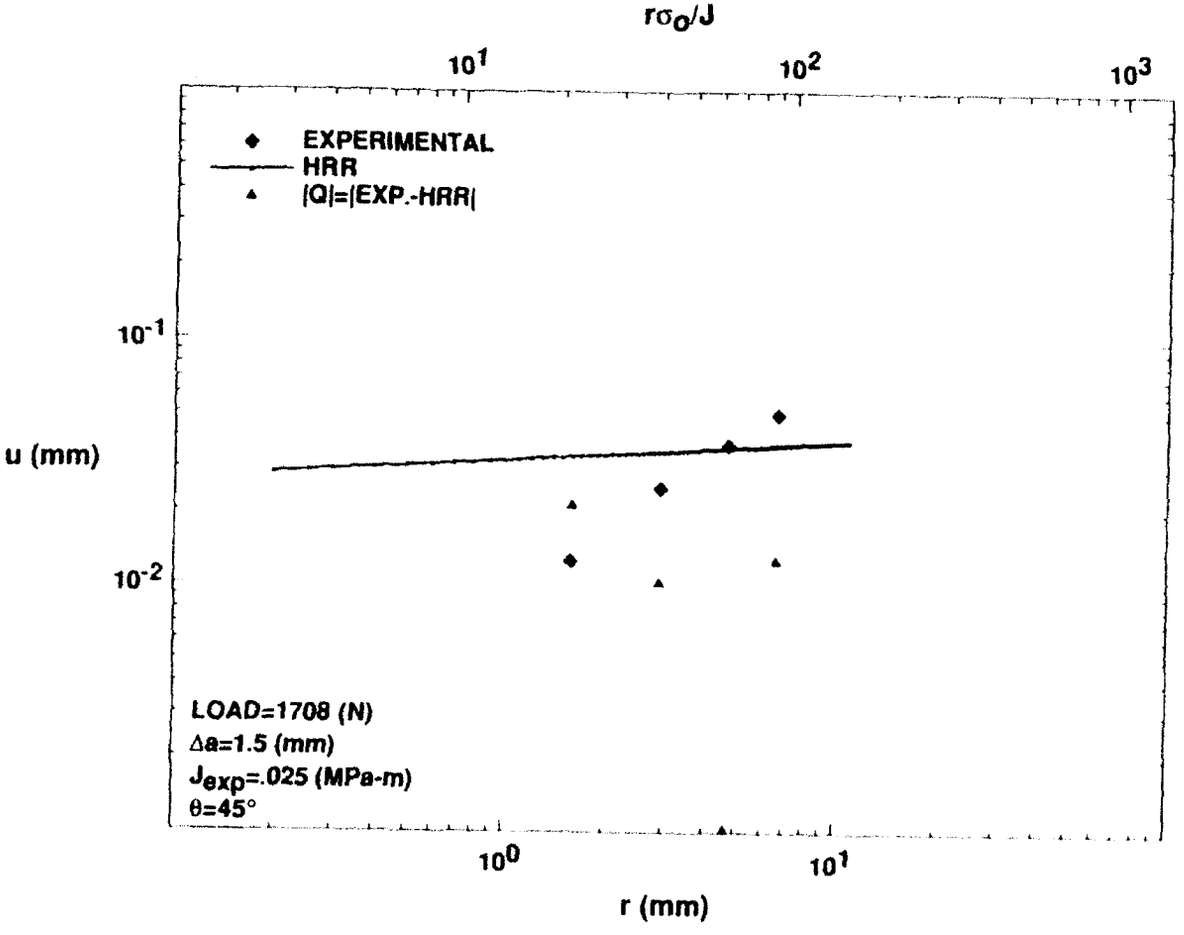

Fig. 7b. u-displacement in 2024-T3 SEN specimen.

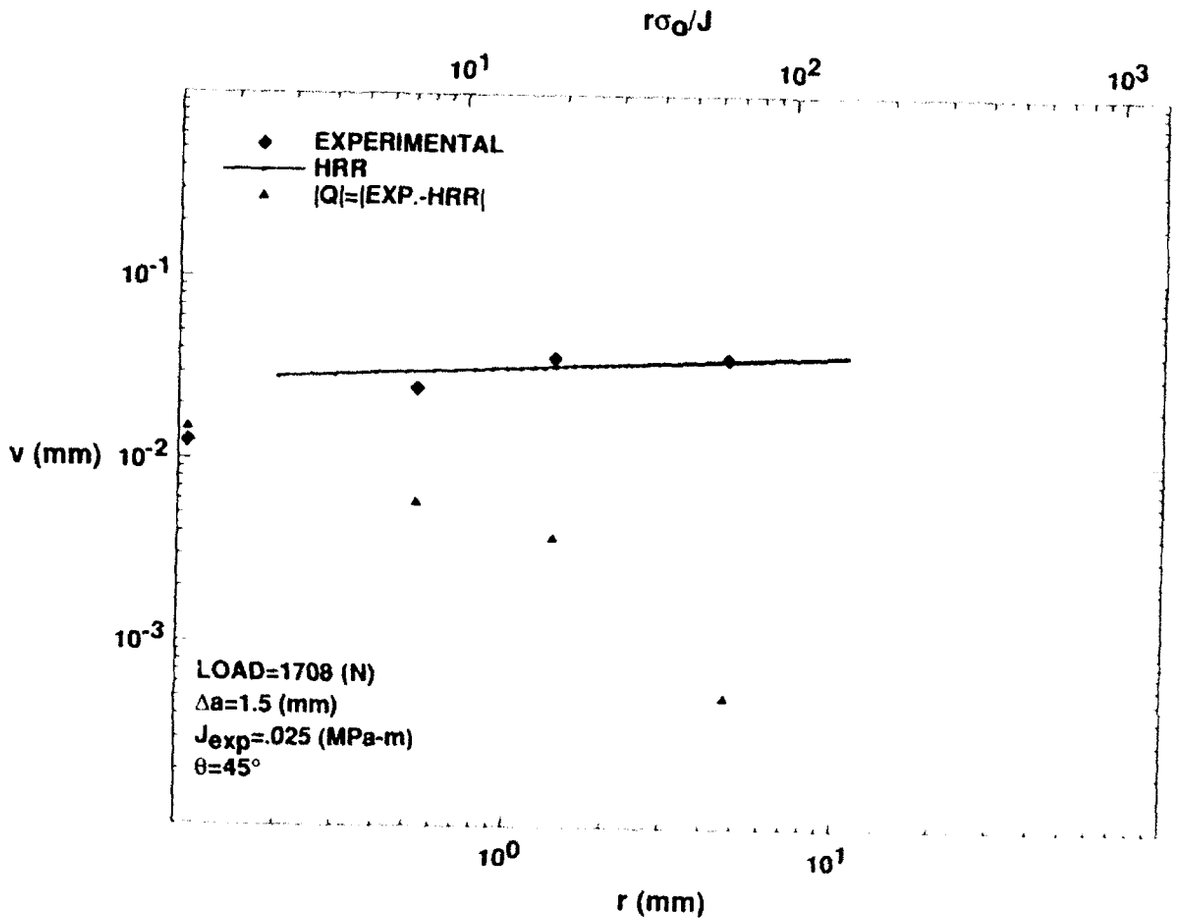

Fig. 8a. v-displacement in 2024-T3 SEN specimen.

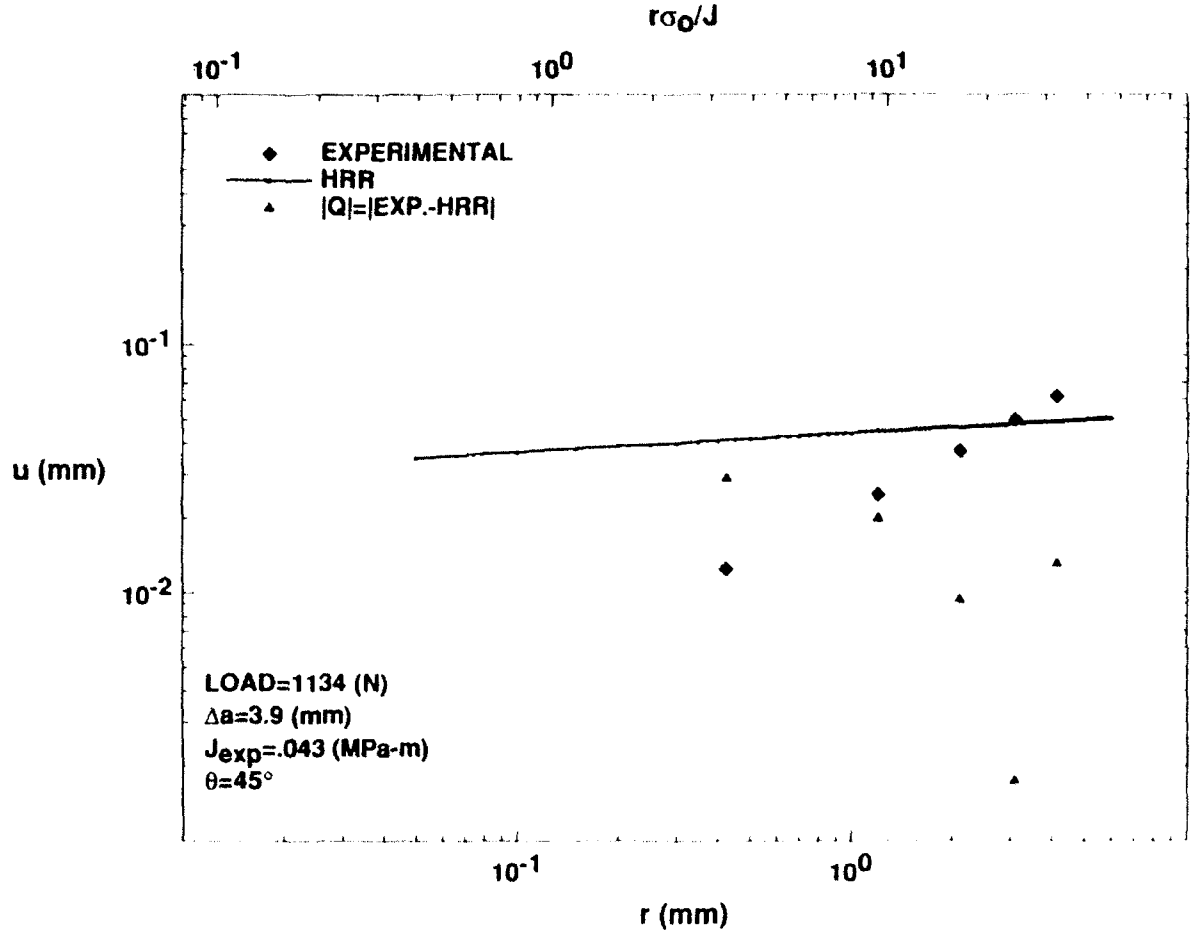

Fig. 8b. u-displacement in 2024-T3 SEN specimen.

Unclassified

SECURITY CLASSIFICATION OF THIS PAGE

REPORT DOCUMENTATION PAGE

Form Approved OMB No. 0704-0188

1a. REPORT SECURITY CLASSIFICATION: unclassified	1b. RESTRICTIVE MARKINGS: None
2a. SECURITY CLASSIFICATION AUTHORITY	3. DISTRIBUTION/AVAILABILITY OF REPORT: Unrestricted
2b. DECLASSIFICATION/DOWNGRADING SCHEDULE	
4. PERFORMING ORGANIZATION REPORT NUMBER(S): UWA/DME/TR-93/71	5. MONITORING ORGANIZATION REPORT NUMBER(S)
6a. NAME OF PERFORMING ORGANIZATION: University of Washington; 6b. OFFICE SYMBOL (If applicable)	7a. NAME OF MONITORING ORGANIZATION
6c. ADDRESS (City, State, and ZIP Code): Seattle, WA 98195	7b. ADDRESS (City, State, and ZIP Code)
8a. NAME OF FUNDING/SPONSORING ORGANIZATION: Office of the Chief of Naval Research; 8b. OFFICE SYMBOL (If applicable): ONR	9. PROCUREMENT INSTRUMENT IDENTIFICATION NUMBER: NT 4324/69-11a12
8c. ADDRESS (City, State, and ZIP Code): 800 N. Quincy Street, Arlington, VA 22217-5000	10. SOURCE OF FUNDING NUMBERS: PROGRAM ELEMENT NO. / PROJECT NO. / TASK NO. / WORK UNIT ACCESSION NO.

11. TITLE (Include Security Classification): Two-Parameter Crack Tip Field Associated with Stable Crack Growth in a Thin Plate-A Hybrid Analysis.

12. PERSONAL AUTHOR(S): G.B. May, F.X. Wang, A.S. Kobayashi

13a. TYPE OF REPORT	13b. TIME COVERED	14. DATE OF REPORT (Year, Month, Day)	15. PAGE COUNT
Technical Report	FROM June 92 TO Apr 93	April 1993	18

16. SUPPLEMENTARY NOTATION

17. COSATI CODES: FIELD	GROUP	SUB-GROUP

18. SUBJECT TERMS (Continue on reverse if necessary and identify by block number): Ductile fracture, moire interferometry, stable crack growth, J-integral, HRR field, Q-parameter.

19. ABSTRACT (Continue on reverse if necessary and identify by block number)

Moire interferometry was used to determine the two orthogonal displacement fields surrounding a stably growing crack in a thin 2024-T3 aluminum alloy, single edge notched (SEN) specimen. The measured displacements were used to compute the J-integral and the associated HRR and the second order Q displacement fields. Also a 2-D elastic-plastic finite element model of the fracturing specimen was executed in its generation mode to compute the crack tip displacement field and the J-integral for small crack extension. The numerically computed and experimentally derived J-values agreed prior to crack extension but differed increasingly with stable crack growth. The HRR and measured v-displacements agreed well but significant difference between the HRR and measured u-displacements was noted. Thus the Q component of the v-displacement was negligible but the corresponding u-component varied nonlinearly with radial distance from the crack tip.

20. DISTRIBUTION/AVAILABILITY OF ABSTRACT	21. ABSTRACT SECURITY CLASSIFICATION
☒ UNCLASSIFIED/UNLIMITED ☐ SAME AS RPT ☐ DTIC USERS	unclassified
22a. NAME OF RESPONSIBLE INDIVIDUAL: A.S. Kobayashi	22b. TELEPHONE (Include Area Code): (206)543-5433 / 22c. OFFICE SYMBOL: ME

DD Form 1473, JUN 86 — Previous editions are obsolete. — SECURITY CLASSIFICATION OF THIS PAGE